EasyChair Preprint

№ 6699

CPFD Modeling to Study the Hydrodynamics of an Industrial Fluidized Bed Reactor for Alumina Chlorination

Zahir Barahmand, Chameera Jayarathna and Chandana Ratnayake

September 26, 2021

CPFD modeling to study the hydrodynamics of an industrial fluidized bed reactor for alumina chlorination

Zahir Barahmand[1] Chameera Jayarathna[2] Chandana Ratnayake[1,2]

[1] Department of Process, Energy and Environmental Technology, University of South-Eastern Norway
zbarahmand@gmail.com
[2] SINTEF Tel-Tek, SINTEF Industry, Porsgrunn, Norway

Abstract

Aluminum is one of the most used metals. Since aluminum has a unique combination of appealing properties and effects, it allows significant energy savings in many applications, such as vehicles and buildings. Although this energy-saving leads to lower CO_2 emissions, the production process of aluminum still dramatically impacts the environment.

The process used exclusively in the aluminum industry is the Hall-Héroult process with a considerable carbon footprint and high energy consumption. As the best alternative, Alcoa's approach (which is not industrialized yet) is based on the chlorination of processed aluminum oxide, reducing the traditional method's negative impacts.

Further to Alcoa's effort, this study aims to investigate the possibility of a new low-carbon aluminum production process. This aim can be achieved by designing an industrial fluidized bed reactor with an external (due to high corrosion inside the reactor) gas-solid separation unit. The aim is to handle 0.6 kg/s of solid reactants and produce aluminum chloride as the main product. The research focuses on determining the best bed height based on the available reaction rates, choosing the best reactor dimension to reduce particle outflow under isothermal conditions (700°C). Autodesk Inventor® and Barracuda® are used for 3D modeling of the reactor and CFD simulation for multiphase (solid-gas) reactions, respectively. Although results have shown that the bed aspect ratio (H/D; H- bed Height and D- bed Diameter) does not affect the reaction, it highly affects the reactor's hydrodynamics and particle outflow. The final design shows the best hydrodynamics belongs to bed aspect ratio equal to 2.

Keywords: CPFD simulation, Bubbling regime, Fluidized bed reactor, Reactor design, Alumina Chlorination

1 Introduction

Aluminum is now the second most used metal globally (Bray, 2021). This is because aluminum has a unique combination of appealing properties and functionalities allowance for significant energy savings in many applications, such as vehicles and buildings. Besides, recycled aluminum is highly energy-efficient, using only 5% of primary production energy (Mapping Resource Prices: The Past and the Future, 2012). Although this energy-saving leads to lower CO_2 emissions, the production process of aluminum still has a massive impact on the environment (The Aluminium Effect, 2021). One of the aluminum industry's key targets (such as many other sectors) has remained aluminum manufacturing with the lowest carbon footprint possible, thanks to growing concern about global climate change (Adoption of the Paris Agreement, 2015). The industrial sector contributes approximately 21% of global greenhouse gas (GHG) emissions, with aluminum industries accounting for 1.0 percent (11.5 tons of CO_2 per ton of aluminum) (Clemence, 2019), and many key players in the global aluminum sector have taken the lead and made progress in reducing CO_2 emissions in their smelting operations. This becomes more important when the significant increase in the global aluminum market size from around 150 billion dollars in 2019 to 250 billion by 2027 with a compound annual growth rate of 5.7% during the period is reported (Aluminium Market Size, Trends | Global Industry Forecast [2027], 2021).

The process which is used almost exclusively in the aluminum industry is the Hall-Héroult process. This process has turned aluminum metal into a commodity product since its invention in 1886 (Kovács et al., 2020). Alumina is dissolved in a cryolite bath in this continuous process, and aluminum is produced by electrolysis. In this cryolite-alumina melt electrolysis, aluminum oxide is dissolved in molten cryolite (Na_3AlF_6) and afterward electrolytically reduced to aluminum at almost 960°C. Carbon anodes are used in the process, consumed during electrolysis, resulting in the formation of CO_2. This process suffers from relatively high heat loss from the electrolytic cells and increased CO_2 emissions from the anodes, even though manufacturers have gradually improved their production processes. Besides, the Hall-Héroult process moves down to its potentially lowest energy consumption and CO_2 emissions during decades (Prasad, 2000).

Alternative aluminum processing strategies have been under intense investigation due to the comparatively high energy usage and carbon footprint

associated with anode consumption (Thonstad, 2001). In continuation of this, in 1973, an innovative process was introduced by Alcoa Corporation, and it had several advantages compared to the commonly used method (Hall-Héroult) at that time (*National Fuels and Energy Conservation Act, S. 2176*, 1973). Alcoa's process is based on the chlorination of processed aluminum oxide. The chlorination process has the advantages of being more compact and operating at a lower temperature than the Hall-Héroult process, normally 700°C. The chemical carbon footprint of the two processes, however, is similar since aluminum chloride is created by carbochlorination of aluminum oxide, which includes aluminum oxide reacting with carbon (C) and chlorine gas (Cl_2) to form aluminum chloride ($AlCl_3$) and CO_2. As a result, the same amount of CO_2 is extracted per kilogram of aluminum in classical electrolysis. However, there are some significant differences although that make this process fascinating. First, this process does not necessitate the use of pure aluminum oxide as a raw material exclusively.

Consequently, the Bayer process could be skipped, eliminating the issue of disposing of vast amounts of red sludge (*Survey of Potential Processes for the Manufacture of Aluminium*, 1979). Second, carbochlorination can result in relatively high CO_2 concentrations in the process gas, making CO_2 capture and storage easier to implement (Øye, 2019). The third, the mechanical properties of carbon, which is merely a chemical reactant in aluminum chloride production by chlorination, are unnecessary. As a result, biocarbon can be used instead of coke from petroleum refineries, required by the Hall-Héroult process requires anodes with high mechanical strength and density (Øye, 2019).

Around the time of the Alcoa process's implementation, a great deal of work was conducted on both the process and the chlorination of raw materials. Later, interest somewhat waned, but it has recently reappeared. Theoretically, many minerals containing sufficient amounts of aluminum can be directly chlorinated. So naturally, minerals with such a weak thermodynamic bond to aluminum, such as clay minerals bauxite and kaolinite, as well as hydrated aluminum sulfates, are preferred (Peterson & Miller, 2007).

Until now, fluidized bed technology has been studied in a wide range of applications. Even though it is a well-known technology, designing such a reactor with ideal and realistic operating conditions continues to be a challenge without advanced numerical calculations. The complexity of hydrodynamics and the uncertain nature of the particles' behavior with their enormous influential characteristics in the fluidized bed reactor make this engineering process complex (Barahmand, Aghaabbasi, et al., 2021). A highly corrosive environment inside the reactor adds the design further challenges.

2 Hydrodynamics

The hydrodynamic models depict solid motion and distribution, gas-solid mixtures, bubble size, velocity, growth, the relationship between the bubble and emulsion phases, and mass and heat transfer processes (Yang, 2003). The balance of forces between particles and gas velocity defines the hydrodynamics of a fluidized bed. It is possible to set the required fluidization regime by adjusting the gas velocity (Philippsen et al., 2015). The fixed bed has a low gas velocity, which keeps the bed static. The minimal fluidization regime is the fluidization regime's beginning point. When the gas velocity exceeds the minimum fluidization velocity, the bubbles form, causing flow instability. When the gas velocity exceeds the terminal velocity, the pneumatic transfer of particulates occurs, and it is employed in circulating fluidized beds (Kunii & Levenspiel, 1991).

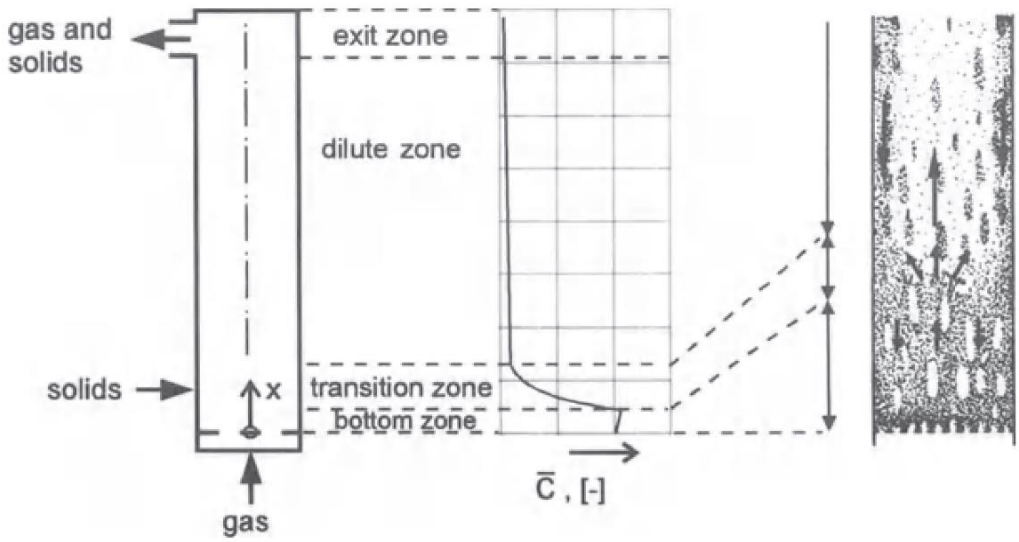

Figure 1. Solids motion and of different solids volume fractions zones (Horio, 1997)

Because of interactions between the gas and solid phases, fluidized beds have highly complex hydrodynamics. The movements of gases and solids are tough to define and explain. Hydrodynamics in a fluidized bed reactor deals with the mechanics of gas-solid suspensions and the hydrodynamic properties of gas-solid contacts. The dilute suspension's clustering nature, first observed from the relatively high gas-solid slip velocity, has been the most significant point of concern from a theoretical perspective. On the other hand, the impact of structural factors such as column diameter, wall shape, gas distributor design, exit configuration, solid separation and recycling equipment, as well as operating conditions, on the performance of circulation systems are the main hydrodynamic concerns from an engineering standpoint which is relatively interrelated with scientific aspects (Horio, 1997).

Any mechanical interactions in the model must be considered in a mathematical model to correctly simulate all of the flow processes associated with gas-solid flows. These interactions, which are dependent on the mean and fluctuating components of the gas and solid velocity fields, are described by (Sinclair & Jackson, 1989) as 1) the interaction between average gas and solid velocity results in the drag force between the two phases, 2) the gas-phase Reynolds stresses are created by the interaction of average and fluctuating gas velocities, 3) the interaction between average and fluctuating solid velocities in the solid assembly that causes stresses., and 4) the interaction of particles with a fluctuating gas velocity, resulting in an interfacial flux of kinetic energy correlated with arbitrary motion.

The properties of the particles have a significant effect on fluidization. Geldart (Geldart, 1973) divided particle behavior in fluidization into four categories, which are now generally recognized and applied in fluidized bed modeling.

- Group A: The particles are small (30–150 μm) and have a low density (1.4 g/cm^3). The fluidization is simple, smooth, and consistent. It allows operating with modest gas flows while still controlling the size and speed of the bubbles.
- Group B: Medium-diameter particles (40–500 μm) having a density of 1.4 – 4 g/cm^3. For high gas flow rates, fluidization is appropriate. Bubbles emerge at the onset of fluidization and expand rapidly.
- Group C: Particles with a diameter of less than 30 μm. Fluidization is a complex process.
- Group D: Particles that are dense and big (d > 500 μm). Fluidization is complex and uneven, making spouted beds suitable.

2.1 Particle motion and solids mixing mechanisms

Studying fluidized bed hydrodynamics (Hartge et al., 1988; Zhang et al., 1991) has indicated that the solids volume concentrations in the fluidized bed reactor can be classified into mainly four regions (Figure 1). First, cross-sectional average solids volume concentrations of usually 0.1 to 0.2 characterize the bottom region, where solid particle acceleration occurs. Next, a dilute region follows the transition zone, occupying most of the riser height and marked by low solids volume concentrations (> 1%). Finally, the exit geometry governs the fluid dynamics throughout the exit zone at the reactor's top (smooth or abrupt exit) (Horio, 1997).

2.1.1 Particle motion in the dense bed

In a previous work (Svensson et al., 1993), it is reported that the dense bottom zone of a fluidized bed experiences hydrodynamic activity similar to bubbling or turbulent fluidized beds, with fluidization gas flowing through the reactor's bottom typically in the form of voids, based on pressure variations at the bottom. These voids break and push solids into the transfer zone as they hit the bottom zone's surface. Since there have not been enough local experiments on solids mixing in the bottom zone of a fluidized bed, it is safe to conclude that the mixing processes are identical to those in bubbling fluidized beds. According to (Kunii & Levenspiel, 1991), "the transport in the wakes of rising voids is the essential mixing mechanism."

2.1.2 Particle motion in the dilute zone

The presence of two phases (lean and dense phase) can describe the dilute region. According to studies in local hydrodynamics (Hartge et al., 1988), the lean phase comprises an upward-moving dilute suspension, while the dense phase comprises downward traveling particle clusters. The dense phase is made near the riser wall for the most part and has solids concentrations at least marginally more significant than the lean phase. For the sake of convenience, the dense phase is often believed to be constrained to a layer near the wall. Figure 2 demonstrates radial profiles of local solids mass fluxes collected by a suction probe as an example of solids motion in the dilute zone (Kruse & Werther, 1995). Reduced solids fluxes[1] are plotted against r/R to demonstrate the results. The upward solids mass fluxes are highest at the reactor's core and decline as they approach the sidewall, while the downward mass fluxes are the opposite. Under these operating conditions, comparatively high downward-moving mass fluxes have been observed at the wall.

The presence of a radial profile of local average solids velocities is another feature of the dilute region. It is

[1] Averaging the local disparity between upward and downward mass fluxes across the cross-sectional area.

reported that the reactor's core has the highest solids velocities (Figure 3), with mean solids velocities of 1.5 to 2 times the superficial gas velocity (Yang et al., 1992). Showing a dominant downward movement of solid particles near the sidewall, negative values are registered. In 1992 (Rhodes et al., 1992), a high-speed video camera to perform a more thorough analysis of the acceleration of downward flowing solids in regions near the wall was used. At velocities ranging from -0.3 to -0.4 m/s, high-density particle swarms were observed descending in contact with the wall. Falling solids were observed to drop with a velocity of -1 m/s as strands a few millimeters from the wall.

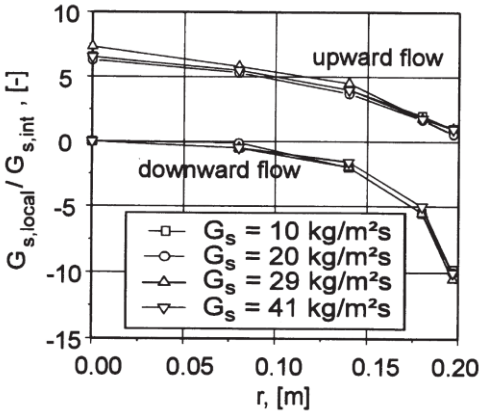

Figure 2. Radial profiles of solids mass fluxes (Horio, 1997)

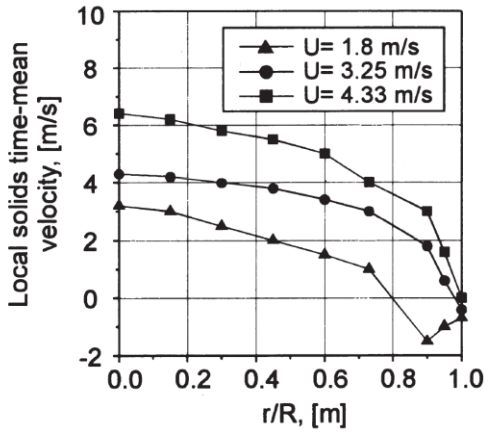

Figure 3. Radial profiles of solids velocities (Horio, 1997)

2.1.3 Particle motion in the transition zone

A transition from the dense bottom zone to the dilute zone happens in this zone, with low solids volume concentrations of solid and the gas phase (Senior & Brereton, 1992). Significant volumes of solids are released from the bottom zone into the transition zone through bursting voids. Solids from the dilute zone are carried back into the zone by dropping clusters. As a consequence, this is a high-intensity mixing region. Solid particles mix in the transfer region; on the other hand, the phenomenon has not yet been studied separately (Horio, 1997).

2.1.4 Particle motion in the exit zone

In the literature, two primary forms of exit geometries have been identified as smooth and abrupt exits. The first is a smooth bent pipe from the top of the fluidized bed reactor to the gas separation unit (cyclone) entry, with no impact on the reactor's flow regime, and the second geometry includes a sharp 90° take-off below the reactor's end cap. Experiments using an abrupt exit (Mabrouk et al., 2008) have revealed increasing solids concentrations at the top of the riser. This effect is caused by solids colliding with the reactor's end cap. Heavier particles, which cannot follow the gas flow through the outlet, are mirrored at the riser's top, allowing solids to accumulate in this region (Horio, 1997).

2.2 Heterogeneous particles fluidization

Solid segregation happens when different solids with varying sizes and densities are fluidized, closely related to solids mixing. Solids segregation in bubbling fluidized beds has gained much interest recently (Nienow, 1985). The consequences of segregation are commonly unfavorable and harm hydrodynamics inside the reactor (Barahmand et al., 2021c).

2.3 Particle's classification

In (Zhang et al., 2014), The fluidization state has been described using a generalized flow regime diagram with the Reynolds number as a function of the Archimedes number. As seen in Figure 4, the Archimedes number (or Geldart classification) and the height to bed diameter ratio may be used to classify diverse materials properly. These experiments have studied the effect of different H/D based on hundreds of powders in different Geldart classifications on the fluidized bed hydrodynamics. In practice, there are, in many cases, there are different alumina types in a process that have different physical properties (Barahmand et al., 2021c). Hence, considering and studying the possibility of segregation is essential for designers.

3 CPFD simulations and discussion

The main goal of the present study is to simulate the alumina chlorination reaction under an isothermal condition at 700℃ in a simple cylindrical fluidized bed reactor and study the effect of different bed aspect ratios (H/D) on the reaction conversion rate and hydrodynamics of the system. The reactor height has been chosen relatively high enough to avoid particle escape in fluidization. The alumina size and reaction

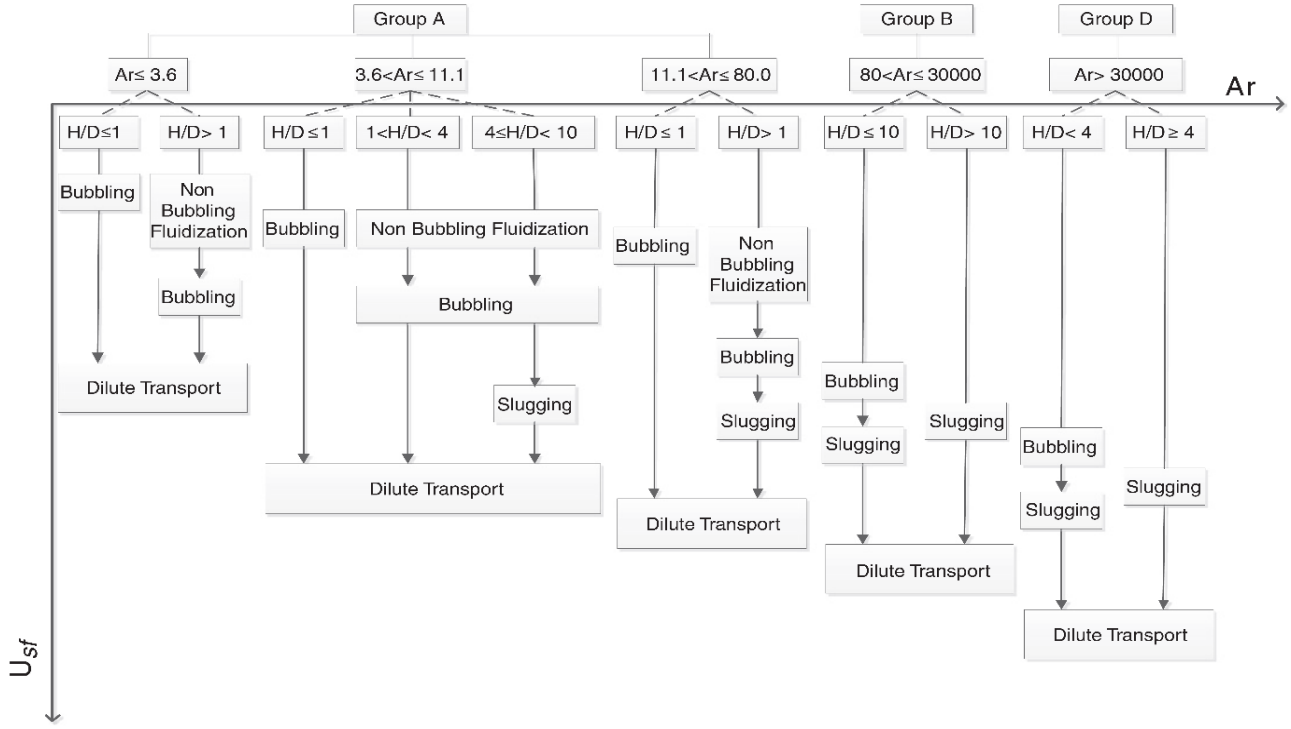

Figure 4. Block flow regime diagram for different particle classification in a fluidized bed (Shaul et al., 2012)

kinetics are based on (Barahmand et al., 2021b). The Archimedes number for the alumina sample can be calculated as 3.59 (Geldart group A). Therefore, H/D below and above unity has been considered into simulations. This study investigates the effect of different bed aspect ratios and operating pressures on the reaction conversion rate. The overall reaction and mass balance are given in equations (1) and (2).

$$Al_2O_3 + 3Cl_2 + 3CO \rightarrow 2AlCl_3 + 3CO_2 \qquad (1)$$

3.1 Bed aspect ratio (H/D)

To study the effect of bed aspect ratio on reactor hydrodynamics and reaction efficiency, different H/Ds have been chosen (0.5, 1, 1.5, 2, 2.5, and 3).

Figure 5 shows the initial bed at the time 0 for 6 different cases. Almost 1500 seconds after fluidization, the system experiences a steady-state. The expanded beds are shown in Figure 6, where the red color represents the solid region in the bed. In all cases, the bed's solid regions cause the fluid to escape through the area between the reactor wall and the bed.

The Cl_2 average mass concentrations and mole fractions at the outlet are given in Table 1. As shown in Figure 7, the highest and lowest Cl_2 concentration belongs to H/D equal to 3 and 1, respectively. Thus, the results show that the bed aspect ratio (above unity) harms the reaction conversion.

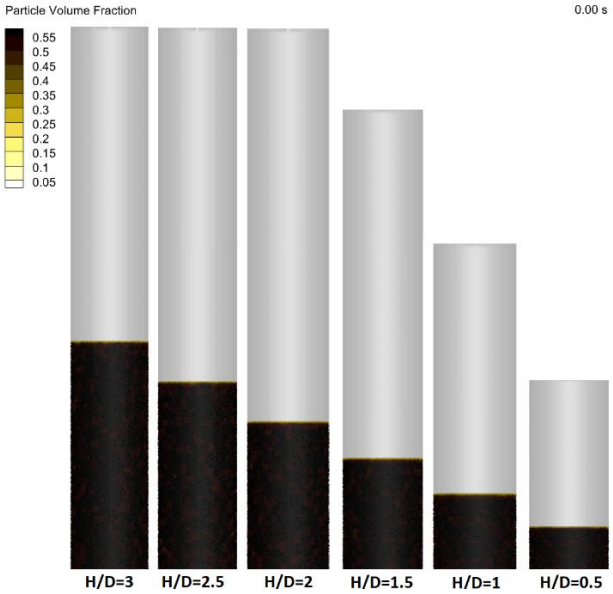

Figure 5. Initial bed for different H/Ds

Table 1. Cl_2 concentration and mole fraction at the outlet

H/D	Mass Concentration (g/m^3)	Mole Fraction
3	38.15	0.0375
2.5	21.2	0.0161
2	19.2	0.0146
1.5	5.6	0.0043
1	0.62	0.0005
0.5	1.96	0.0015

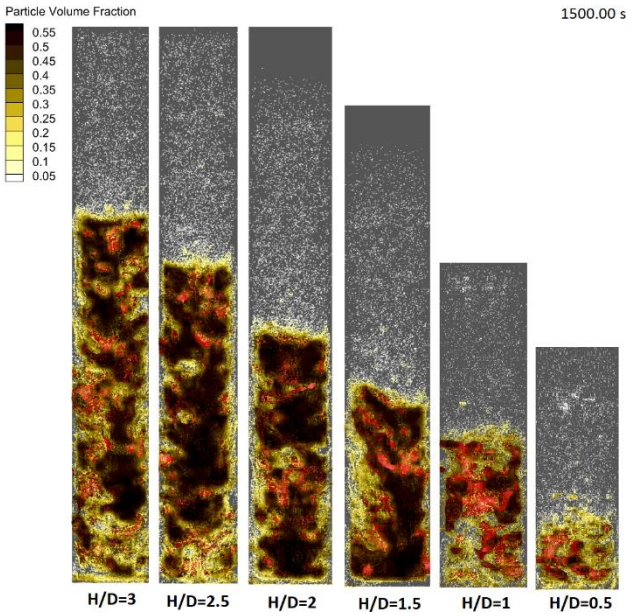

Figure 6. Solid regions in the bed at steady-state

Although the H/D equal to unity shows the best performance in reaction conversion, to choose a proper bed aspect ratio, it is necessary to consider the whole hydrodynamics of the bed (Barahmand et al., 2021a, 2021b). Too low H/D can cause channeling, and it may reduce the reaction efficiency. As a result, Cl_2 concentration at the reactor outlet may increase. Even a tiny amount of Cl_2 at the outlet could cause problems if there is no purification process on Cl_2. Too high H/D may also cause channeling because of creating strong solid regions in the bed. Simultaneously, too high H/D will increase energy consumption significantly due to the increased pressure drop of the reactor.

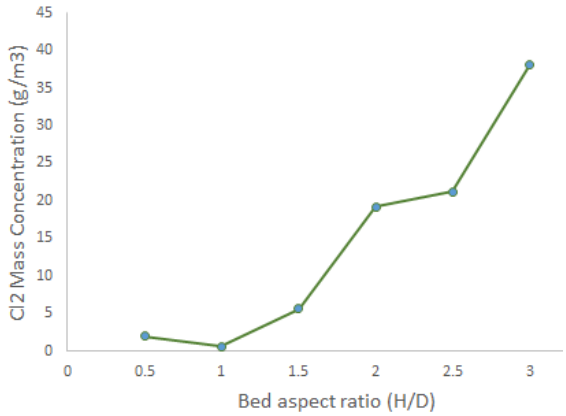

Figure 7. Average Cl_2 concentration in the outlet vs. H/D

3.2 Pressure Effect

In the next step, the present work aims to study the effect of the operating pressure on the reactor's chemical performance. The outlet pressure boundary condition directly affects the fluid's superficial velocity for a certain fluid mass flow rate. Choosing H/D=1, several simulations have been done in different conditions. Each simulation has a duration of at least 1500 seconds to reach the pseudo-steady-state. As seen in Figure 8, the average Cl_2 mass concentration in the outlet increases by increasing the outlet pressure. Therefore, it can be concluded that it is favorable to operate the reactor with the lowest pressure to have better reaction conversion.

There is a negative correlation between the reactor's outlet pressure and the reaction conversion. Studying the effect of outlet pressure on Cl_2 mass concentration illustrates that the minimum concentration belongs to the range when outlet pressure is between 1 and 2 bars.

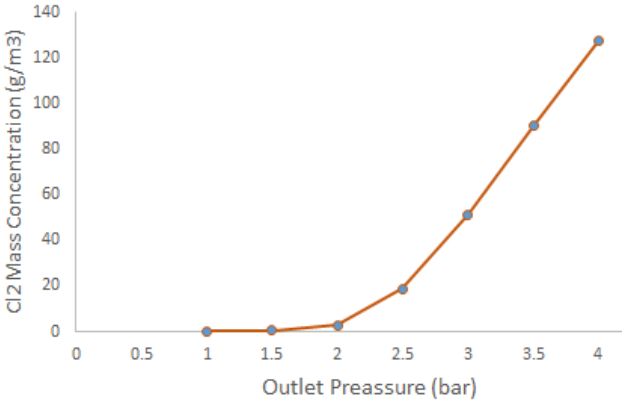

Figure 8. The effect of the pressure on the Cl_2 concentration

4 Conclusions

As simulation results show, almost all the Cl_2 are consumed within the first meter of the reactor, which means the current range of bed and reactor height may not be fully activated in an actual chlorination process. However, the H/D value has a significant role when it comes to suitable hydrodynamics of the reactor. Therefore, selecting the reactor specification for good hydrodynamics of the gas-solid fluidized bed reactor is very important. Too low and high H/D can cause channeling. A low H/D may reduce the reaction efficiency. Too high H/D may also cause channeling because of creating strong solid regions or increasing energy consumption significantly. The results show that the reactor performs best (minimum Cl_2 mass concentration at the outlet) when the outlet pressure ranges between 1 and 2 bars.

Considering all factors to ensure the reliable and effective operation of the fluidized bed reactor (such as hydrodynamics, change in Cl_2 concentration over height, and particle outflow, etc.), the suitable height to diameter ratio (H/D) can be considered as 2. Results of further simulations related to the selected H/D ratio are reported by (Barahmand, 2021).

References

Adoption of the Paris Agreement (FCCC/CP/2015/L.9/Rev.1). United Nations, 2015. https://unfccc.int/resource/docs/2015/cop21/eng/l09r01.pdf

Aluminium Market Size, Trends | Global Industry Forecast [2027], 2021.

Z. Barahmand. *Design of an Industrial Chlorination Reactor Using CPFD Simulations* [Master Thesis]. University of South-Eastern Norway, 2021.

Z. Barahmand, O. Aghaabbasi, E. K. L. Rustad, J. L. Salcido, C. Jayarathna, and C. Ratnayake. Designing of a medium-scale circulating fluidized bed reactor for chlorination of processed aluminum oxide. *In Proceedings - 1st SIMS EUROSIM Conference on Modelling and Simulation*, Finland, 2021.

Z. Barahmand, C. Jayarathna, and C. Ratnayake. CPFD simulations on a chlorination fluidized bed reactor for aluminum production: An optimization study. *In Proceedings - 1st SIMS EUROSIM Conference on Modelling and Simulation*, Finland, 2021a.

Z. Barahmand, C. Jayarathna, and C. Ratnayake. Study of the thermal performance of an industrial alumina chlorination reactor using CPFD simulation. *In Proceedings - 1st SIMS EUROSIM Conference on Modelling and Simulation*, Finland, 2021b.

Z. Barahmand, C. Jayarathna, and C. Ratnayake. The effect of alumina impurities on chlorination in a fluidized bed reactor: A CPFD study. *In Proceedings - 1st SIMS EUROSIM Conference on Modelling and Simulation*, Finland, 2021c.

E. L. Bray. *Aluminum Statistics and Information*. United State National Minerals Information Center, 2021. https://www.usgs.gov/centers/nmic/aluminum-statistics-and-information

C. Clemence. *Leaders Emerge In The Aluminium Industry's Race To Zero Carbon*. Aluminium Insider, 2019. https://aluminiuminsider.com/leaders-emerge-in-the-aluminium-industrys-race-to-zero-carbon/

D. Geldart. Types of gas fluidization. *Powder Technology*, 7(5), 285–292, 1973. doi:10.1016/0032-5910(73)80037-3.

E. Hartge, D. Rensner, and J. Werther. Solid concentration and velocity patterns in circulating fluidized bed. In P. Basu & J. F. Large (Eds.), *Circulating Fluidized Bed Technology*, pages 165–180. Pergamon, 1988. doi:10.1016/B978-0-08-036225-0.50020-4

M. Horio. *Circulating Fluidized Beds* (J. R. Grace, A. A. Avidan, & T. M. Knowlton, Eds.). Springer Netherlands, 1977. doi:10.1007/978-94-009-0095-0_2

A. Kovács, C. Breward, K. Einarsrud, S. Halvorsen, E. Nordgård-Hansen, E. Manger, A Münch, and J. Oliver. A heat and mass transfer problem for the dissolution of an alumina particle in a cryolite bath. *International Journal of Heat and Mass Transfer*, 162, 120232, 2020. doi:10.1016/j.ijheatmasstransfer.2020.120232

M. Kruse and J. Werther. 2D gas and solids flow prediction in circulating fluidized beds based on suction probe and pressure profile measurements. *Chemical Engineering and Processing: Process Intensification*, 34(3), 185–203, 1995. doi:10.1016/0255-2701(94)04004-4

D. Kunii, O. Levenspiel. *Fluidization Engineering*. Butterworth-Heinemann, 1991.

R. Mabrouk, J. Chaouki, and C. Guy. Exit effect on hydrodynamics of the internal circulating fluidized bed riser. *Powder Technology - POWDER TECHNOL*, 182, 406–414, 2008. doi:10.1016/j.powtec.2007.07.008

Mapping resource prices: The past and the future. ENV.G.1/FRA/20410/0044; pages 370. ECORYS, 2012.

National Fuels and Energy Conservation Act, S. 2176. U.S. Government Printing Office, 1973.

A. W. Nienow. Fluidization of dissimilar materials. *Fluidization*, 357–381, 1985.

B. Øye, B. Could the chloride process replace the Hall-Héroult process in aluminium production? *SINTEFblog*, 2019, March 28. https://blog.sintef.com/sintefenergy/energy-efficiency/could-the-chloride-process-replace-the-hall-heroult-process-in-aluminium-production/

W. S. Peterson and R. E. Miller. *Hall-Heroult Centennial: First Century of Aluminum Process Technology*, 2007.

C. Philippsen, A. Vilela, and L. Zen. Fluidized bed modeling applied to the analysis of processes: Review and state of the art. *Journal of Materials Research and Technology*, 4(2), 208–216, 2015. doi:10.1016/j.jmrt.2014.10.018

S. Prasad. Studies on the Hall-Heroult aluminum electrowinning process. *Journal of the Brazilian Chemical Society*, 11, 245–251, 2000. doi:10.1590/S0103-50532000000300008

M. Rhodes, H. Mineo, and T. Hirama. Particle motion at the wall of a circulating fluidized bed. *Powder Technology*, 70(3), 207–214, 1992. doi:10.1016/0032-5910(92)80055-2

R. Senior and C. Brereton. Modelling of circulating fluidised-bed solids flow and distribution. *Chemical Engineering Science*, 47(2), 281–296, 1992. doi:10.1016/0009-2509(92)80020-D

J. Sinclair, and R. Jackson. *Gas-particle flow in a vertical pipe with particle-particle interactions*, 1989. doi:10.1002/AIC.690350908

Survey of potential processes for the manufacture of aluminium (ANL/OEPM-79-4). Little (Arthur D.), Inc., Cambridge, MA (USA), 1979.

A. Svensson, F. Johnsson, and B. Leckner. Fluid-dynamics of the bottom bed of circulating fluidized bed boilers. *In Proceedings - 12th International Conference on Fluidized-*Bed Combustion, 2, 887–897, 1993.

The Aluminium Effect—European Aluminium. 2021. https://european-aluminium.eu/about-aluminium/the-aluminium-effect/

Thonstad, J. (2001). *Aluminium Electrolysis: Fundamentals of the Hall-Héroult Process*. Aluminium-Verlag.

M. Van de Velden, J. Baeyens, J. Degrève, and J. Seville. The residence time distribution of the gas phase in circulating fluidized beds (CFB). *In Proceedings - European Congress of Chemical Engineering*, 16–20, 2007.

W. Yang. *Handbook of Fluidization and Fluid-Particle Systems*. CRC Press, 2003.

Y. Yang, Y. Jin, Z. Yu, and Z. Wang. Investigation on slip velocity distributions in the riser of dilute circulating fluidized bed. *Powder Technology*, 73(1), 67–73, 1992. doi:10.1016/0032-5910(92)87008-X

H. Zhang, L. Shu, and S. Liao. Generalized Trapezoidal Fuzzy Soft Set and Its Application in Medical Diagnosis. *Journal of Applied Mathematics*, 2014, e312069, 2014. doi:10.1155/2014/312069

W. Zhang, Y. Tung, F. Johnsson. Radial voidage profiles in fast fluidized beds of different diameters. *Chemical Engineering Science*, 46(12), 3045–3052, 1991.